# **Photoconduction in Aromatic Hydrocarbons**

**Abstract:** Photoconduction has been observed in single crystals of benzene, naphthalene, biphenyl and pyrene using the pulse technique. Experimental procedures have been found for the purification and crystal growth of the materials that produce specimens whose charge carrier lifetimes are sufficiently long to allow the measurement of drift mobilities, and thus to determine the number of charge carriers produced per pulse. A single-photon generation mechanism was observed only in pyrene. The other materials exhibited a photogeneration mechanism that depended quadratically on light intensity and was determined to be exciton-exciton collision ionization.

#### Introduction

Studies of the intrinsic photogeneration of charge carriers in pure organic materials have been performed primarily on crystalline anthracene. Many different mechanisms of intrinsic photogeneration have been found for this material and these have been reported only in the last five years, subsequent to the first observation [1] of single-photon carrier production (which begins about 4 eV above the ground state). The evolution of the study of these mechanisms has resulted in a standard experimental arrangement for which the different mechanisms and their efficiencies can be readily determined. In spite of the availability of these tools, studies on the intrinsic photogeneration of charge carriers in organic materials other than anthracene are practically nonexistent. Single-photon intrinsic generation has been reported in tetracene [2] and pyrene [3] but data were obtained only by dc measurements, which are complicated by electrode effects. Of the many multiple photon-exciton photogeneration processes observed in anthracene, none has been reported in other organic materials.

In this paper we report the observation of intrinsic photoconduction in the aromatic hydrocarbons benzene, naphthalene, biphenyl and pyrene. The results are interpreted in terms of those mechanisms already observed for anthracene. Since these may not be familiar, a short discussion of the mechanisms is given in terms of the type of experiment being reported here.

#### Photoconduction in anthracene

The feature of organic materials such as the aromatic hydrocarbons that makes them unusual is the participation of the Frenkel excitons in the photoconduction process. These excitons are derived from excited states present in the free molecule and are only slightly displaced from them in energy  $(10^{-2} \text{ to } 10^{-1} \text{ eV})$  in the crystal. Only the lowest energy exciton state of a given multiplicity (either singlet or triplet for the closed shell systems discussed here) is relatively long lived  $(10^{-9} \text{ to } 10^{-7} \text{ sec for singlets})$ and  $10^{-2}$  to  $10^{-1}$  sec for triplets) and capable of neutral energy migration in the crystal. This energy migration is not restricted to crystals but also appears in disordered systems [4]. In anthracene the lowest lying exciton states (3.1 and 1.8 eV for singlet and triplet, respectively) are well below the photoconduction threshold of about 4.0 eV; thus charge-carrier generation occurs, in the absence of impurities, only when the crystals are excited into higher energy states. The higher energy states are unstable (10<sup>-12</sup> to 10<sup>-14</sup> sec lifetime) and rapidly lose energy via intramolecular radiationless transitions (internal conversion) to the lowest lying exciton states. Those initial states with energies above the conduction band can also autoionize to give free carriers in competition with the radiationless process. No direct experimental evidence is available as to the degree of electron-hole delocalization of the highenergy initial states, but the high efficiency of internal conversion and the low efficiency of free-carrier production indicate that these states should be considered to be localized, as is the lowest lying exciton state (i.e., a Frenkel exciton).

The photogeneration process for a single-photon mechanism is illustrated in Fig. 1. Absorption of light results in the production of an unstable exciton state with energy greater than the band gap. The state is unstable with respect to two processes: a fast radiationless deactivation

27

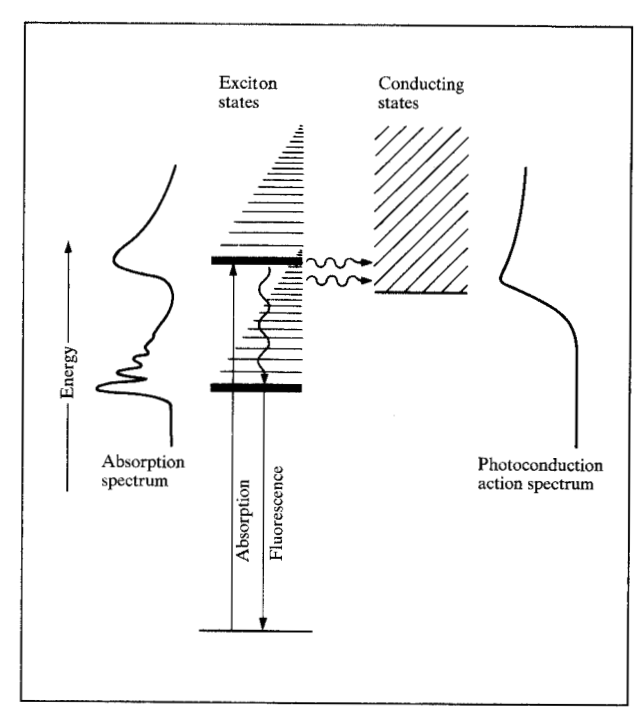


Figure 1 Schematic illustration of a single-photon autoionization process in an organic material.

or internal conversion to the lowest energy exciton state (wavy vertical arrow) and an autoionization process yielding free carriers (wavy horizontal arrows).

The problem of a bound exciton state undergoing simultaneous internal conversion and autoionization has been treated theoretically by Jortner [5]. By using a modification of Fano's theory [6], Jortner took into account the interaction between the bound state  $\phi_A$ , the quasicontinuum of vibronic states  $\phi_i$  (vibrationally excited states built on lower energy electronically excited states) and the continuum of conducting states  $\phi_E$ . The resulting expression for the wave function  $\psi$  of the unstable state is just a simple superposition of states,

$$\psi = a(E)\phi_A + \sum_i b_i \phi_i + \int C_{E'} \phi_{E'} dE'. \qquad (1)$$

The coefficients  $b_i$  contain the coupling matrix elements  $\langle \phi_i | H | \phi_A \rangle$ , which are usually just vibrational electronic matrix elements, and a density of vibronic states. Similarly the coefficients  $C_{E'}$  contain the Coulomb interaction  $V_E = \langle \phi_E | H | \phi_A \rangle$ , which determines the autoionization process, and the density of conducting states. The quantum yield of charge carrier production is determined by the ratio of the coefficients (branching ratio). In anthracene the quantum yield over the energy range 4 to 6 eV is about  $10^{-4}$  carrier/photon, whereas the quantum yield for production of fluorescent excitons (3.1 eV) is close to

unity, which indicates the dominant role of the radiationless decay.

The many different mechanisms reported for anthracene can be thought of as just different ways in which the metastable autoionizing states are initially formed. These mechanisms for anthracene are described in Table 1 and it is to be expected that some of the mechanisms will be found in other materials. Essentially every process involving excitons and phonons that together have a total energy greater than 4 eV has been reported to give rise to carrier production in anthracene. These processes include

- 1. Direct single-photon ionization of the ground state [1]
- 2. Direct two-photon ionization of the ground state [7]
- 3. Photoionization of singlet excitons [8]
- 4. Photoionization of triplet excitons [9]
- 5. Singlet exciton-singlet exciton collision ionization [10]
- 6. Singlet exciton-triplet exciton collision ionization [11].

Of course, the nature of the autoionizing states will differ according to the mode of excitation. For example, the photoionization of a triplet exciton produces autoionizing states that are primarily triplet in character, whereas photoionization of the ground state produces autoionizing states that are primarily singlet in character. The internal conversion, and thus the branching ratio, could be very different for those two types of state even though the energies could be equal.

It is interesting to note in Table 1 that the branching ratio for a single-photon ionization of the ground state is similar to that for direct two-photon ionization of the ground state. The absorption selection rules predict that the former mode of excitation produces crystal states of ungerade symmetry and the latter, gerade symmetry.

## Experiment

# • Pulse technique

The experiment that has yielded the most reliable data on organic materials has been the pulsed-light technique [13]. The experimental arrangement is depicted in Fig. 2. In this arrangement a short pulse of light is incident on, and strongly absorbed by, a crystal that is sandwiched between two electrodes, one of which is transparent. In our particular experiments the crystal is insulated from the electrodes by thin quartz discs (blocking electrodes) to prevent photoinjection of carriers into the crystal by the electrodes. The light duration is about 0.5 µsec, which is much shorter than the typical transit times of 20 to 100 µsec. The light forms charge carriers within the extinction depth (typically 10<sup>-5</sup> cm) and, depending on the polarity of the applied field, either holes or electrons drift through the crystal. The passage of carriers through the crystal leads to a characteristic current pulse, under non-space-charge conditions, the width of which equals

Table 1 Charge-carrier generation mechanisms observed in anthracene.

Mechanism	Light intensity dependence	Wavelength dependence	Efficiency	Remarks
Single-photon extrinsic	Linear	Reproduces crystal absorption spectrum; $N \propto k$ (extinction depth)	Quantum yield: $\Phi(e^+) = 10^{-4} \text{ to } 10^{-2}$ hole/photon	Observed only for hole production; therefore $\Phi(e^+) \neq \Phi(e^-)$ . See Ref. 12.
Single-photon intrinsic	Linear	4-eV threshold 4.0 4.4 5.6 eV	$\Phi(e^{+}) = \Phi(e^{-}) = 10^{-4}$ at 298°K; $E = 10^{4} \text{ V/cm}$	No extinction depth dependence, as indicated by lack of a polarization effect. The yield of 3.1-eV excitons is essentially unity.
Direct two-photon	Quadratic	2-eV threshold	Two-photon cross section for carrier generation: $10^{-30}$ cm-sec	Two-photon cross section for 3.1-eV exciton generation: $10^{-26}$ cm-sec. See Ref. 7.
Singlet exciton- singlet exciton collision ionization	Quadratic	$N \propto k$	Carrier-generation rate constant: 0.9 × 10 <sup>-12</sup> cm <sup>3</sup> -sec <sup>-1</sup>	Exciton-exciton total annihilation rate constant:  1.5 × 10 <sup>-8</sup> cm <sup>3</sup> -sec <sup>-1</sup> . See Ref. 10.
Singlet exciton- triplet exciton collision ionization	Quadratic	Fixed wavelength experiment; $h_{\nu} = 1.8 \text{ eV}$	Carrier-generation rate constant: 10 <sup>-12</sup> cm <sup>3</sup> -sec <sup>-1</sup>	Triplet exciton (1.8 eV) produced by intersystem crossing of singlet exciton (3.1 eV). See Ref. 11.
Single-photon ionization of a singlet exciton	Cubic	Fixed wavelength experiment; $h\nu = 1.8 \text{ eV}$	Ionization cross section: $2 \times 10^{-19} \text{ cm}^2$ [8(a)] $0.6 \times 10^{-19} \text{ cm}^2$ [8(b)]	Proportional to $I^3$ instead of $I^2$ since the singlet excitons are produced by two-photon absorption. See Refs. 8(a) and 8(b).
Single-photon ionization of a triplet exciton	Quadratic	Fixed wavelength experiments; $h\nu = 2.6 \text{ eV}$ $h\nu = 2.35 \text{ eV}$	Ionization cross section: $4 \times 10^{-21} \text{ cm}^2$ $5 \times 10^{-22} \text{ cm}^2$	See Ref. 9. See Ref. 7.

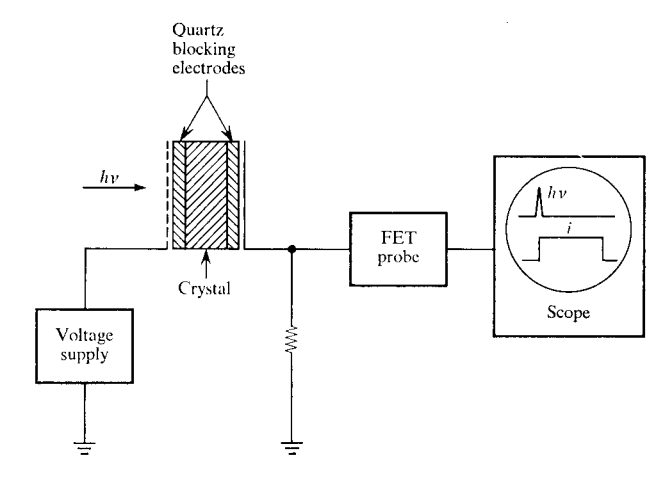
the transit time and the area of which represents the number of mobile charges produced. Any bulk trapping of the carriers is reflected in a decay of the current.

The use of blocking electrodes requires that the dark conductivity be very small [less than  $10^{-16}$  (ohm-cm)<sup>-1</sup>] and that the carrier lifetimes be long enough to enable a determination of the mobility. These two requirements are rather severe for organic crystals and are the principal reason why there is a dearth of experimental data. These requirements have been overcome for the materials mentioned in this paper.

## • Purification of materials

Benzene (Phillips research grade, 99.94%) was purified by zone refining, followed by fusion over cesium according to the method of Colson and Bernstein [14], and further zone refining. Naphthalene (Eastman 168) was purified by zone refining, followed by fusion over potassium according to the method of Hanson and Robinson [15], and further zone refining. Biphenyl (Eastman 721) was purified in a manner identical to that for naphthalene.

Figure 2 Experimental arrangement for pulsed-light irradiation and observation of waveform.



Pyrene (Princeton Organics, 99.999 mole% purity) was zone refined.

Two types of sample cell were used in our experiments. One cell was used for crystals that were cut from large

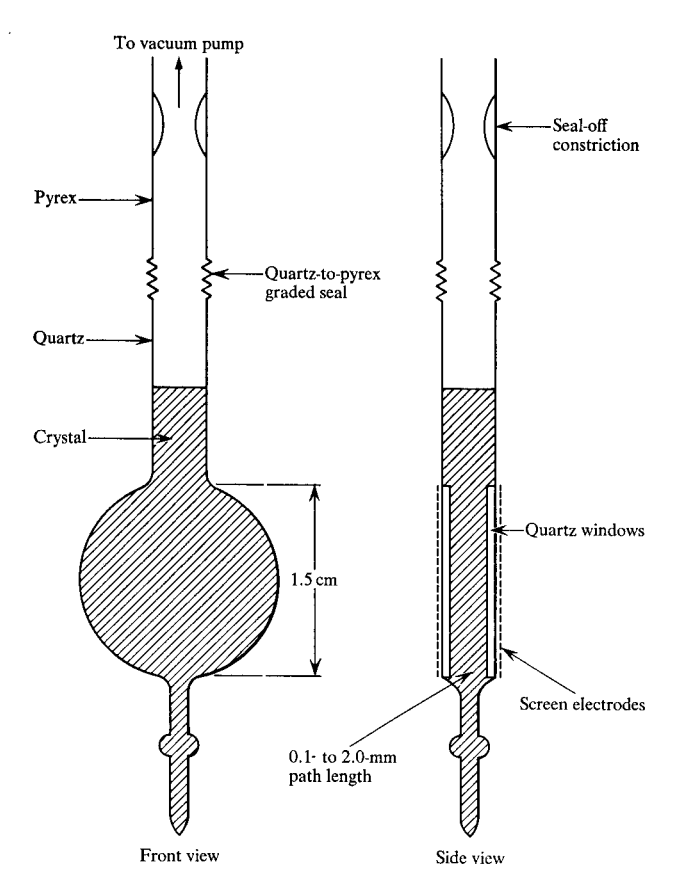


Figure 3 Fused-quartz photoconduction cell.

ingots grown either from the melt (naphthalene and biphenyl) or from the vapor (pyrene). The crystals, typically 1 cm<sup>2</sup> in area and 1 mm thick, were sandwiched between a metallic collecting electrode and a transparent front electrode consisting of a fine metallic screen insulated by a quartz cover slip.

The second cell, shown in Fig. 3, is a modified fused-quartz spectroscopic cell [16]. In this cell the crystals were grown from the melt *in situ* between the quartz discs under high vacuum. The electrodes were then applied to the outside of the cell. This type of cell represents a simple experimental approach to the production of the clean crystal surfaces that are necessary to eliminate extrinsic carrier production caused by impurities (such as air) at the surface.

### **Results**

### • Pyrene

Photoconduction was observed in pyrene for incident radiation of wavelengths less than 3300 Å. The trapping lifetime of the charge carriers was 15 µsec for holes and electrons in crystals grown from the vapor at a maximum temperature of 107°C. The carrier lifetimes were suf-

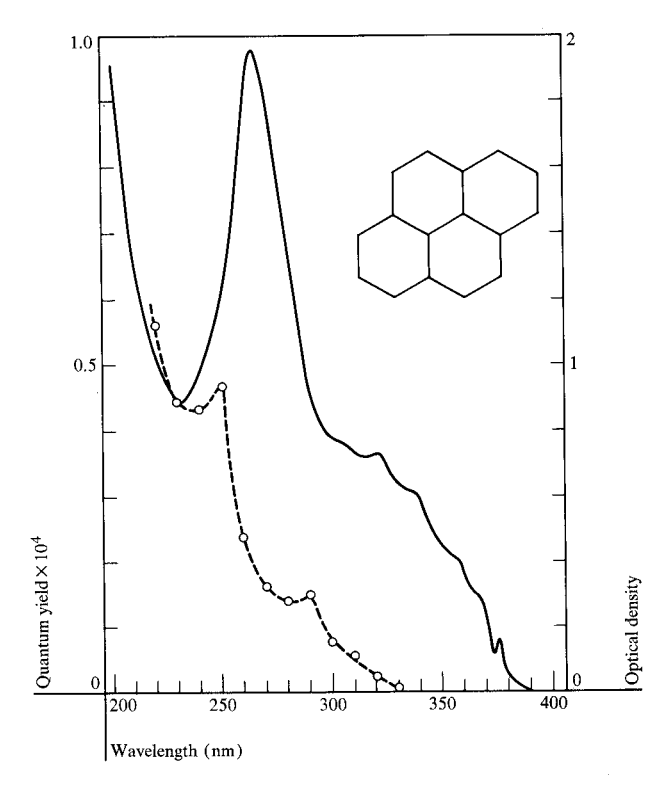


Figure 4 Photoconduction action spectrum (circles, dashed line) of crystalline pyrene. The resolution is 10 nm. The absorption spectrum (solid line) was taken with a resolution of 0.1 nm on a crystal approximately 1  $\mu$ m thick.

ficiently long to enable us to measure a transit time and thus to determine the number of carriers from the current transients. The number of carriers produced depends linearly on light intensity, and essentially equal numbers of holes and electrons are produced per incident photon. The action spectrum is shown in Fig. 4. The onset of photoconduction does not coincide with the crystal absorption edge at 4000 Å. These observations are similar to those of Chaiken and Kearns [3], who used dc measurements, except that here we did not observe large positive currents at 3500 Å due to hole injection at the positive electrode, and we can determine an absolute quantum yield. The quantum yield observed at 2500 Å is 2.5  $\times$ 10<sup>-5</sup> at 296°K in a field of 9000 V/cm. The process is, by analogy with anthracene, a direct, intrinsic, singlephoton ionization and as such assigns the conduction band a maximum energy of 3.8 eV above the valence band.

#### • Naphthalene

Photoconduction was observed in this material when it was irradiated at a wavelength less than 3300 Å. The crystals, grown from the melt, exhibited carrier trapping lifetimes in excess of 500  $\mu$ sec for both holes and electrons. Typical photocurrent transients are shown in Fig. 5.

The number of carriers produced varied quadratically with light intensity (the slope of N vs I is 1.8 at 2900 Å). It has been shown by Braun [10] that the wavelength dependence of an  $I^2$  process for strongly absorbed light can be used to differentiate between exciton-exciton collision and exciton-photoionization mechanisms since only the former process should show a generation rate proportional to the extinction depth (i.e., the action spectrum should resemble the crystal absorption spectrum). The wavelength dependence observed is shown in Fig. 6 (normalized to equal light intensity) along with the crystal absorption strength, which indicates that the mechanism here is one of exciton-exciton collision ionization. Our experiments cannot distinguish the type of exciton involved except to eliminate the possibility of two triplets colliding, since in that case charge carriers would be produced long after the termination of the flash (due to the long triplet lifetime) and this effect is not observed here. The possibility of singlet-triplet collision ionization cannot be eliminated as a mechanism without obtaining better time resolution experiments. These in fact have recently been done on naphthalene by Braun and Dobbs [17], whose results eliminate the participation of triplets in the photogeneration process.

The exciton-exciton collision ionization rate constant  $\beta$ , neglecting diffusion of excitons, was determined from the equation

$$N = \frac{1}{2}\beta \tau^2 k w I_0^2, \tag{2}$$

where N is the number of carriers,  $\tau$  is the exciton lifetime  $(10^{-7} \text{ sec})$ , k is the extinction coefficient, w is the lamp duration, and  $I_0$  is the light intensity. The number obtained is  $1.1 \times 10^{-14} \text{ cm}^3\text{-sec}^{-1}$ .

# • Biphenyl

This material is similar to naphthalene in its optical characteristics and also its electrical properties. The carrier lifetimes are 200 and 100  $\mu$ sec for electrons and holes, respectively, which again permit us to determine transit times. Photoconduction was observed for strongly absorbed light with a quadratic dependence on light intensity. The normalized wavelength dependence is shown in Fig. 7 along with the absorption strength. By analogy with the results on naphthalene, the mechanism in biphenyl appears to be singlet exciton-exciton collision ionization. The rate constant was estimated to be  $6 \times 10^{-14} \, \mathrm{cm}^3$ -sec<sup>-1</sup>, which is similar to that of naphthalene.

## • Benzene

Photoconduction was observed in single crystals of benzene, but only with great difficulty. Although the electron trapping lifetimes are very long (200  $\mu$ sec), the hole lifetimes are very short (less than 1  $\mu$ sec), so that only electron transit times could be observed. The production of free

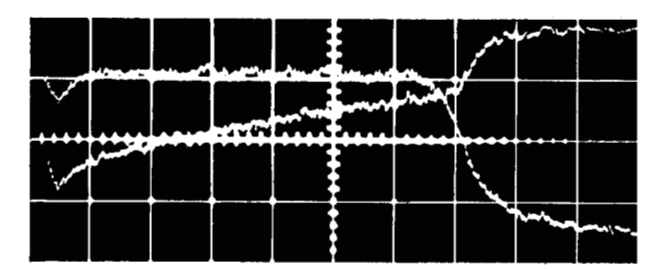
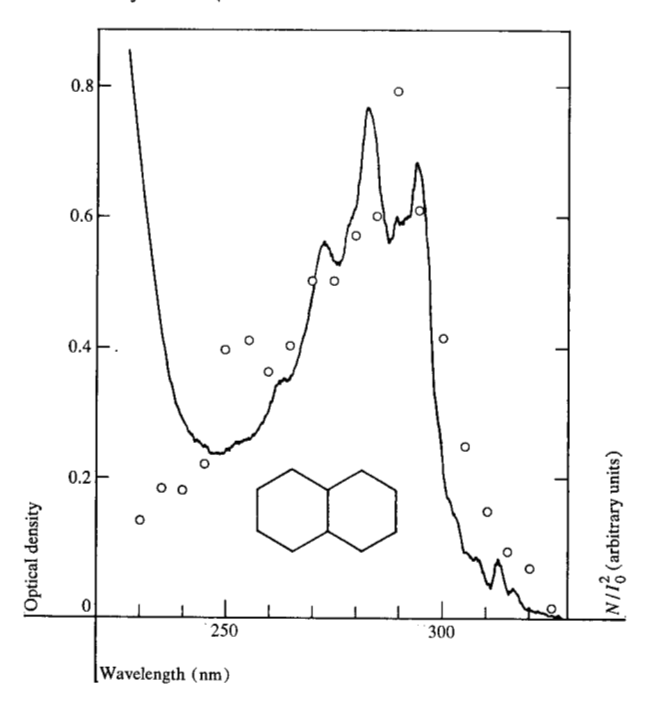


Figure 5 Typical photocurrent transients in naphthalene. The positive transient corresponds to hole motion and shows no trapping, whereas the negative transient indicates that half of the electrons are trapped in this crystal. The electron and hole transit times are identical and yield a mobility of  $0.4~\rm cm^2/V$ -sec for carriers moving perpendicular to the ab plane. The vertical scale is  $1.2~\rm \times~10^{-8}~A/division$  and the horizontal scale is  $20~\mu sec/division$ ; the electric field strength was  $3000~\rm V/cm$ .

Figure 6 Normalized photoconduction action spectrum (circles) of crystalline naphthalene. The resolution is 10 nm. The experimental results at wavelengths less than 250 nm are unreliable because of the low light intensity. The absorption spectrum (solid line) was taken with a resolution of 0.1 nm on a crystal  $0.2~\mu m$  thick.



electrons is very small and, to induce photoconduction at all, the full spectrum of our lamp had to be used. The poor efficiency of photoconduction eliminated the possibility of obtaining a wavelength dependence, but we were able to determine a quadratic light intensity dependence. Some typical photocurrent transients are shown in Fig. 8. By analogy with biphenyl and naphthalene we expect an exciton collision mechanism, but here an upper limit to the rate constant is  $10^{-16}$  cm<sup>3</sup>-sec<sup>-1</sup>.

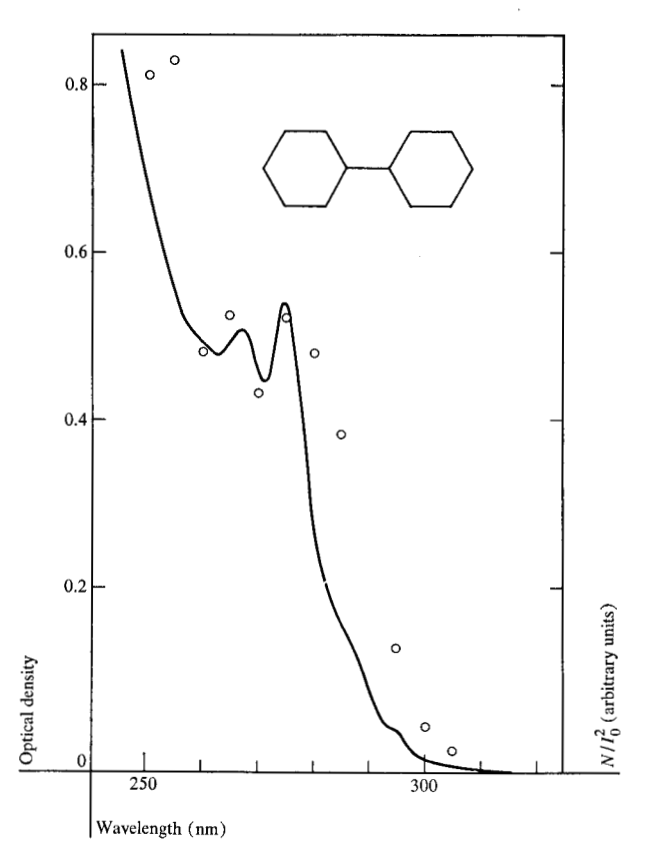
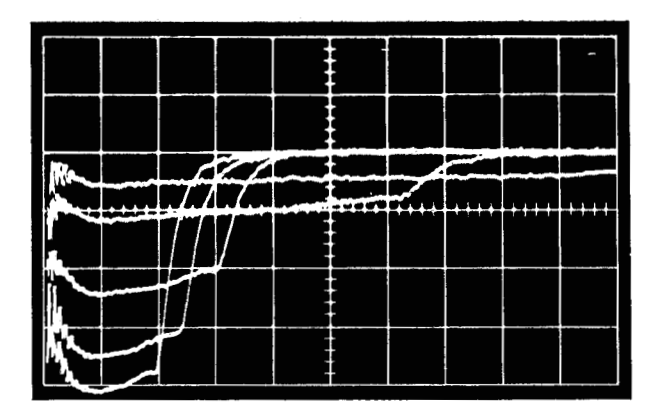


Figure 7 Normalized photoconduction action spectrum (circles) of crystalline biphenyl. The resolution is 10 nm. The absorption spectrum (solid line) was taken with a resolution of 0.1 nm on a crystal approximately 0.2  $\mu$ m thick.

**Figure 8** Typical electron-current transients in crystalline benzene. The vertical scale is  $10^{-8}$  A/division and the horizontal scale is  $10 \, \mu sec/division$ ; the electric field strengths (beginning with lower-left trace) were 5000, 4070, 3230, 1610 and 808 V/cm; the crystal thickness was 2 mm.



## Conclusions

With a reasonable amount of effort and care intrinsic photoconduction can be observed in aromatic hydrocarbons other than anthracene, and crystals can be obtained with sufficient purity to allow the measurement of transit times and thus the number of charge carriers. The mechanisms for charge-carrier formation in the aromatic hydrocarbons are similar to those already observed for anthracene, and this situation serves to establish the generality of those mechanisms. It is not too surprising that for benzene, biphenyl and naphthalene we have observed only exciton-exciton processes and no singlephoton processes in our experiments. The single-photon thresholds are expected to be much higher in energy for these molecules and possibly higher than our experimental limit (5.5 eV) since the free molecule ionization potentials are correspondingly higher. Also, these particular molecules are characterized by an extremely weak lowestsinglet-exciton absorption relative to anthracene, which results in very long lifetimes for the lowest singlet exciton so that collisions are quite probable.

Pyrene is the largest aromatic hydrocarbon for which we have been able to measure transit times. The photoconduction in pyrene is quite similar to that in anthracene, except for the interesting fact that no exciton collision mechanism is observed for this material. The lowest lying exciton state of pyrene is thought to be a dimeric complex that is stable only in the excited state (excimer) and is achieved by a close approach of two molecules after excitation. Such a change in geometry could lead to a self-trapping of the energy and result in a much reduced probability for exciton migration, and thus in a reduced probability for collision, compared with the other aromatic hydrocarbons.

Our results at this point in time for the crystals that show exciton-exciton collision ionization must be considered to be preliminary because the experiments were designed only to establish the mechanism and determine the efficiency. Any further correlation of our experimental results with more basic theoretical concepts is not currently possible since there exists no reliable information on total exciton-exciton annihilation cross sections, exciton diffusion lengths, or even accurate exciton lifetimes for these materials. We are in the process of determining these types of data in our laboratory and are also attempting to prepare suitable samples of larger molecules for similar photoconduction studies.

# Acknowledgment

The author gratefully acknowledges the technical assistance of J. Duran.

#### References

- G. Castro and J. F. Hornig, J. Chem. Phys. 42, 1459 (1965).
- N. Geacintov, M. Pope and H. Kallmann, J. Chem. Phys. 45, 2639 (1966).
- R. F. Chaiken and D. R. Kearns, J. Chem. Phys. 49, 2846 (1968).

- 4. W. Klöppfer, J. Chem. Phys. 50, 2337 (1969).
- 5. J. Jortner, Phys. Rev. Letters 20, 244 (1968).
- 6. U. Fano, Phys. Rev. 124, 1886 (1961).
- 7. F. C. Strome, Jr., Phys. Rev. Letters 20, 3 (1968).
- (a) R. G. Kepler, *Phys. Rev. Letters* 18, 951 (1967);
   (b) E. Courtens, A. Bergman and J. Jortner, *Phys. Rev.* 156, 948 (1967).
- P. Holzman, R. Morris, R. C. Jarnagin and M. Silver, Phys. Rev. Letters 19, 506 (1967).
- C. L. Braun, Phys. Rev. Letters 21, 215 (1968); G. R. Johnston and L. E. Lyons, Chem. Phys. Letters 2, 489 (1968).
- 11. J. Fourny, G. Delacôte and M. Schott, *Phys. Rev. Letters* 21, 1085 (1968).
- O. H. LeBlanc, in *Physics and Chemistry of the Organic Solid State*, edited by D. Fox, M. M. Labes and A. Weissberger, Vol. III, Interscience Publishers, New York 1967.

- 13. R. G. Kepler, Phys. Rev. 119, 1226 (1960).
- S. D. Colson and E. R. Bernstein, J. Chem. Phys. 43, 2661 (1965).
- D. M. Hanson and G. W. Robinson, J. Chem. Phys. 43, 4174 (1965).
- E. R. Bernstein, S. D. Colson, D. S. Tinti and G. W. Robinson, J. Chem. Phys. 48, 4632 (1968).
- 17. C. L. Braun and G. Dobbs, J. Chem. Phys. (to be published).

Received August 11, 1970

The author is located at the IBM Research Laboratory, San Jose, California 95114.